

From comparison to integration: A workflow evaluation of 3D Gaussian splatting and LiDAR point cloud for modern architectural heritage

Yingwen Yu^{a,*}, Edward Verbree^a, Peter van Oosterom^a, Uta Pottgiesser^{a,b}, Yuyang Peng^c, Florent Poux^{d,e}

^a Department of Architectural Engineering and Technology, Faculty of Architecture and the Built Environment, Delft University of Technology, Julianalaan 134, Delft, the Netherlands

^b Institute for Design Strategies (IDS), OWL University of Applied Sciences and Arts (TH OWL), 32756 Detmold, Germany

^c Department of Urbanism, Faculty of Architecture and the Built Environment, Delft University of Technology, Julianalaan 134, Delft, the Netherlands

^d Liège University, GeoScity Lab, Belgium

^e 3D Geodata Academy, Geodata Lab, 200 Rue de la croix nivert 75015, paris, France

ARTICLE INFO

Keywords:

3D Gaussian splatting
LiDAR-based point cloud
Modern architectural heritage
Architectural heritage information infrastructure (AHII)
Real-time visualization
Semantic segmentation

ABSTRACT

This paper investigates the role of 3D Gaussian Splatting (3DGS) within point cloud-dominated workflows for modern architectural heritage digitization. While 3DGS enables real-time, photorealistic visualization, its integration into LiDAR-based documentation pipelines remains underexplored. Using Bouwpub, a modern heritage building in the Netherlands, as a case study, the paper compares 3DGS and LiDAR across data acquisition and preservation, visualization, semantic segmentation, and dissemination. Results show that 3DGS offers superior visual expressiveness and user responsiveness, whereas LiDAR provides greater structural accuracy and segmentation reliability. Based on these findings, two integration strategies are proposed: a Blender-based multi-angle rendering workflow and a Level of Detail 3DGS (LOD3DGS) pipeline. Moving from isolated assessment to applied integration, the study positions 3DGS as a complementary visualization and dissemination module rather than a replacement. This hybrid approach supports immersive, scalable, and semantically enriched digital heritage systems, offering new directions for enhancing both expert documentation and public engagement.

1. Introduction

Modern heritage buildings refer to structures built from the 20th century onwards that possess historical, cultural, artistic, or social significance, reflecting the defining characteristics of their respective periods, as emphasized by ICOMOS¹ and Docomomo International² [1,2]. On the one hand, they form an essential part of humanity's cultural heritage, embodying modern society's diversity and innovation, and warrant dedicated conservation efforts³ [3]. On the other hand, their structural complexity and continued use increase their vulnerability to a range of threats, such as urbanization, natural disasters, and warfare [4–7]. Compared with traditional historical buildings, modern architectural heritage typically features new materials such as reinforced

concrete, steel, and glass curtain walls, resulting in distinct structural forms and material–structure combinations. These buildings often remain in active use, undergoing frequent functional changes that complicate preservation. Additionally, modern heritage generally has lower public recognition, requiring more realistic and immersive digital representation to enhance public engagement. These unique challenges motivate our specific focus on modern architectural heritage in this research [4–7].

To effectively address these complexities, digital archiving has increasingly emerged as a pivotal approach. By enabling precise documentation, preservation, and immersive visual representation, digital archiving ensures that the authenticity, materiality, and unique spatial characteristics of modern heritage buildings are retained and

* Corresponding author.

E-mail addresses: christinayu@tudelft.nl (Y. Yu), e.verbree@tudelft.nl (E. Verbree), p.j.m.vanoosterom@tudelft.nl (P. van Oosterom), u.pottgiesser@tudelft.nl (U. Pottgiesser), y.peng-1@tudelft.nl (Y. Peng), florent@learngeodata.eu (F. Poux).

¹ International Council on Monuments and Sites (ICOMOS). Available online: <https://www.icomos.org/> (Accessed on 16 July 2025).

² Docomomo International. Available online: <https://docomomo.com/organization/> (Accessed on 16 July 2025).

³ UNESCO World Heritage Centre. Available online: <https://whc.unesco.org/> (Accessed on 16 July 2025).

appreciated over time [8–10]. In the past decades, various digital technologies, including photogrammetry, 3D laser scanning using LiDAR (Light Detection and Ranging), and subsequent modeling and visualization techniques, have been employed to support heritage digital archiving [11–13]. These point cloud-based methods have emerged as a dominant and widely accepted workflow in heritage studies [14–16], offering high-precision geometric data that supports accurate documentation [17,18], enables detailed visualization [19–21], facilitates semantic modeling [22–24], and underpins further digital analysis [25,26]. However, conventional point cloud techniques often struggle to capture photorealistic textures and support real-time visualization, capabilities increasingly vital for immersive heritage experiences and broader public engagement [27–29]. Emerging methods such as 3D Gaussian Splatting (3DGS) offer promising alternatives to meet these evolving demands. As an advanced 3D representation technique [30], 3DGS has been suggested to deliver high-fidelity textures and interactive visualization capabilities, potentially complementing traditional point cloud workflows [31–33]. Yet, its application in modern heritage digital archiving remains largely unexplored. Two key research gaps can be identified:

- (a) Although 3DGS shows promising capabilities in photorealistic visualization and rendering efficiency, empirical evidence of its effectiveness in real-world modern heritage contexts, particularly regarding complex geometry and diverse material textures, remains insufficient [34].
- (b) Rather than replacing existing point cloud methods, 3DGS is expected to complement established workflows. However, methodological clarity on how to effectively integrate 3DGS into prevailing LiDAR-based digitization processes, especially concerning visualization, semantic modeling, and dissemination, is currently lacking.

To address the identified gaps, this paper aims to explore the practical application of 3DGS in modern architectural heritage digitization and clarify its integration within existing point cloud-dominant workflows. This overarching aim is divided into three sub-aims: (a) examining the feasibility and potential of applying 3DGS in real-world heritage contexts; (b) positioning 3DGS within current digitization workflows dominated by point clouds; and (c) investigating how 3DGS can enhance existing heritage digitization practices in terms of efficiency and expressiveness.

To achieve these objectives, the paper is structured as follows. First, it reviews existing research on the technical characteristics and applications of LiDAR-based point cloud techniques and 3DGS in heritage digitization. Subsequently, a comparative methodological workflow is applied to a selected case study—Bouwpub, a modern heritage building within the Rijksmonument-listed complex of TU Delft in the Netherlands, representing typical modern architectural heritage.⁴ The comparative analysis primarily addresses three critical aspects of heritage digitization: visualization quality, semantic segmentation, and effective dissemination (Sections 3 & 4). Additionally, the paper briefly describes data acquisition processes and implications for data preservation, although these aspects are not quantitatively compared. Empirical findings clarify the functional role of 3DGS and identify pathways for its effective integration into existing workflows, thus supporting more efficient, realistic, and semantically rich digital heritage practices (Section 5).

This paper contributes to the Architectural Heritage Information Infrastructure (AHII) by demonstrating how 3DGS complements established LiDAR-based approaches. It provides clear guidance for integrating diverse digitization methods, advancing both practical heritage

documentation and effective public dissemination strategies.

2. Related works

This section reviews existing research on point cloud technologies and emerging image-based methods, particularly 3DGS, highlighting their current applications, strengths, and limitations in modern heritage digitization contexts.

2.1. Point cloud technology in modern heritage digitization

Point cloud is a three-dimensional data representation method that captures the spatial morphology of objects by recording XYZ coordinates and color information of their surfaces. It is widely used in the digitization of modern architectural heritage [25,35,36]. The primary methods for acquiring point cloud data include LiDAR scanning and photogrammetry [37–39]. LiDAR obtains high-density point cloud data through laser ranging, while photogrammetry reconstructs point clouds by matching multi-angle images [40]. These data support the entire lifecycle of heritage digitization, from acquisition and modeling to condition assessment, visualization, and dissemination, playing a vital role in documentation, monitoring, analysis, and informed decision-making [41].

- (a) **Data acquisition and digital surveying:** LiDAR and image-based photogrammetry are the two most prevalent methods for generating point clouds. Terrestrial laser scanning (TLS) provides high-precision geometry with sub-centimeter accuracy, making it ideal for documenting complex structures [40,42]. Unmanned Aerial Vehicles (UAV)-based photogrammetry complements TLS by covering inaccessible facades or roof structures [43], while mobile or handheld systems enhance indoor or detailed component capture [44]. These technologies allow the creation of comprehensive digital archives, which are vital for further applications [45,46].
- (b) **Visualization and 3D representation:** Point cloud data supports interactive 3D visualization and spatial inspection. Tools such as Autodesk Recap,⁵ CloudCompare,⁶ and Potree⁷ are commonly used to navigate, annotate, and share point-based representations [47]. However, raw point clouds typically lack texture fidelity and do not inherently represent continuous surfaces, thus posing challenges for immersive applications such as virtual or augmented reality [48,49]. To address this, many studies have highlighted the trade-off between geometric density and rendering efficiency, leading to hybrid visualization strategies [50]. These strategies typically include either direct point cloud rendering enhanced by real-time shaders or indirect visualization through intermediate steps such as surface reconstruction to mesh models [51]. Nevertheless, direct use of raw point clouds remains common in heritage digitization workflows due to their geometric accuracy and minimal data loss [52].
- (c) **Semantic segmentation and modeling:** Beyond geometric visualization, point cloud segmentation enables the conversion of raw spatial data into semantically meaningful architectural elements. Recent advances in deep learning and machine learning have significantly improved the classification of components such as walls, vaults, and windows [53,54]. Subsequently, semantic modeling uses these segmented outputs as a basis or reference to construct structured semantic representations, most notably Historic Building Information Modeling (HBIM). In HBIM workflows, segmented point clouds guide the creation of parametric

⁴ Delft Municipality Open Data Portal. Available online: <https://data.delft.nl/> (Accessed on 16 July 2025).

⁵ Overview | ReCap | Autodesk.

⁶ CloudCompare - Open Source project ([danielgm.net](https://www.danielgm.net)).

⁷ Potree

architectural models, which are further enriched with historical, material, and structural metadata [55,56]. Such HBIM models have proven valuable for condition assessment, restoration planning, and interdisciplinary collaboration [57,58].

- (d) **Digital dissemination and public engagement:** Point cloud-based models increasingly facilitate the dissemination of heritage knowledge to broad audiences. By employing interactive web platforms (e.g., Potree, Sketchfab), virtual reality (VR), augmented reality (AR), and immersive digital exhibitions, these models allow the public to visually explore and experience heritage sites remotely [59]. High-profile initiatives, such as *Digital Dunhuang* and *Virtual Monticello*, demonstrate how point cloud reconstructions significantly enhance global accessibility, offering virtual visits to otherwise fragile, restricted, or remote heritage locations [60,61]. Through immersive storytelling and interactive exploration, these applications actively support heritage education, encourage cultural tourism, and stimulate greater public awareness and engagement in cultural identity and conservation efforts.

Overall, point cloud technology has become the foundational layer of modern heritage digitization, supporting detailed geometric documentation, semantic modeling, and digital dissemination across the full lifecycle of heritage management [27]. However, despite its strengths in precision and structure, point cloud representations often face challenges in achieving high-fidelity surface realism, seamless real-time rendering, and engaging visual storytelling. These limitations have motivated the exploration of emerging methods, such as image-based neural rendering and Gaussian-based techniques, that aim to enhance or complement point cloud workflows in heritage visualization.

2.2. 3D Gaussian splatting in heritage studies

3DGS is a 3D scene representation technique that models spatial radiance using anisotropic Gaussian kernels (Fig. 1). Each Gaussian encodes position, orientation, opacity, and color, enabling smooth surface appearance and real-time rendering without the need for neural network inference. Compared to mesh- or point cloud-based visualization, 3DGS has shown promising photorealism and rendering potential based on calibrated RGB imagery, suggesting suitability for immersive visualization tasks. Yet, systematic empirical evaluation within specific heritage contexts has not been sufficiently explored. [62].

Recent studies have begun to explore its potential in cultural heritage contexts. Clini et al. [63] compared 3DGS with SfM-MVS and NeRF for reconstructing a Romanesque church, indicating preliminary advantages of 3DGS in visual realism and rendering interactivity. Other efforts include the reconstruction of a noble family chapel in Palermo using consumer-grade video and 3DGS for interactive exhibition [64], drone-based neural rendering of remote sites [65], and artistic experiments combining 3DGS with curatorial storytelling in digital heritage narratives [66]. These applications suggest the emerging value of 3DGS in rapid documentation, public engagement, and immersive interpretation, particularly where conventional scanning methods are inaccessible.

Nevertheless, comprehensive empirical assessments validating these advantages across broader heritage scenarios remain absent.

In addition, its integration into established digital heritage workflows remains limited. Existing practices, especially those based on LiDAR point clouds, support accurate geometric documentation, semantic modeling, and structured archiving. In contrast, 3DGS lacks topological and parametric structure and is not readily compatible with HBIM, GIS, or component-based annotation systems. Its current pipeline also provides minimal support for semantic interaction or operational control. These limitations reveal three key research gaps. First, the functional role of 3DGS within point cloud-dominated workflows is not clearly defined, particularly regarding interoperability, rendering layering, and semantic complementarity. Second, the absence of structured metadata and editing control hinders its integration into collaborative or annotation-driven environments. Third, while early demonstrations exist, there is a lack of systematic empirical evaluation of 3DGS specifically in modern architectural heritage, which involves complex materials, hybrid geometries, and continued use, and which presents distinct challenges for documentation and visualization. Bridging these gaps is essential for repositioning 3DGS as a visualization tool and a complementary method in digital heritage practices. Notably, peer-reviewed applications of 3DGS in architectural heritage remain scarce, particularly in cases involving modern materials and large-scale documentation, making this an urgent area for empirical research and methodological development.

2.3. Synthesis and study positioning

Although 3DGS has attracted increasing attention in graphics and neural rendering, its application in architectural heritage digitization remains largely unexplored. Existing uses are limited to small-scale or artistic reconstructions, with no systematic evaluation in structured heritage workflows, especially in modern architectural contexts, where material complexity and spatial scale pose additional challenges. Meanwhile, LiDAR remains the dominant method for geometry-focused heritage documentation, yet it operates separately from emerging image-based rendering techniques. Few studies have assessed how 3DGS and LiDAR perform across comparable tasks, or how their integration could enhance both spatial accuracy and visual expressiveness. To address these gaps, this study evaluates 3DGS within a real-world heritage scenario and explores its role as a complementary visualization layer in LiDAR-based workflows, offering a hybrid approach that bridges geometric precision with real-time visualization and dissemination.

3. Methodology

This paper conducts a comparative investigation of two representative technologies in modern heritage digitization, namely image-based 3DGS and LiDAR-based point clouds, by independently applying each workflow to the same heritage site. The full pipeline is executed for both methods, encompassing data collection and storage, visualization, semantic segmentation, and VR-based dissemination (Fig. 2).

Specifically, data collection and storage underpin accurate

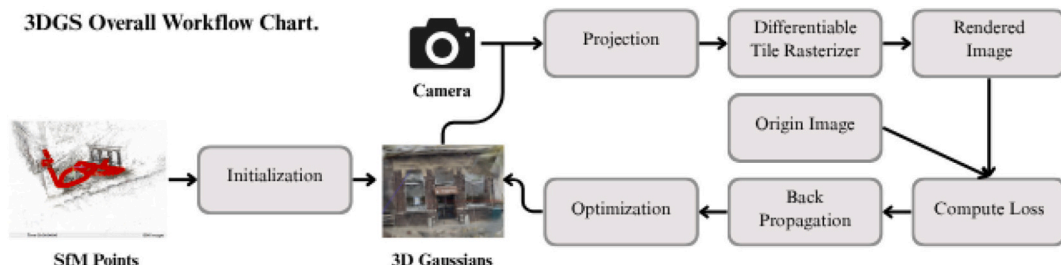


Fig. 1. Standard workflow for 3DGS [67].

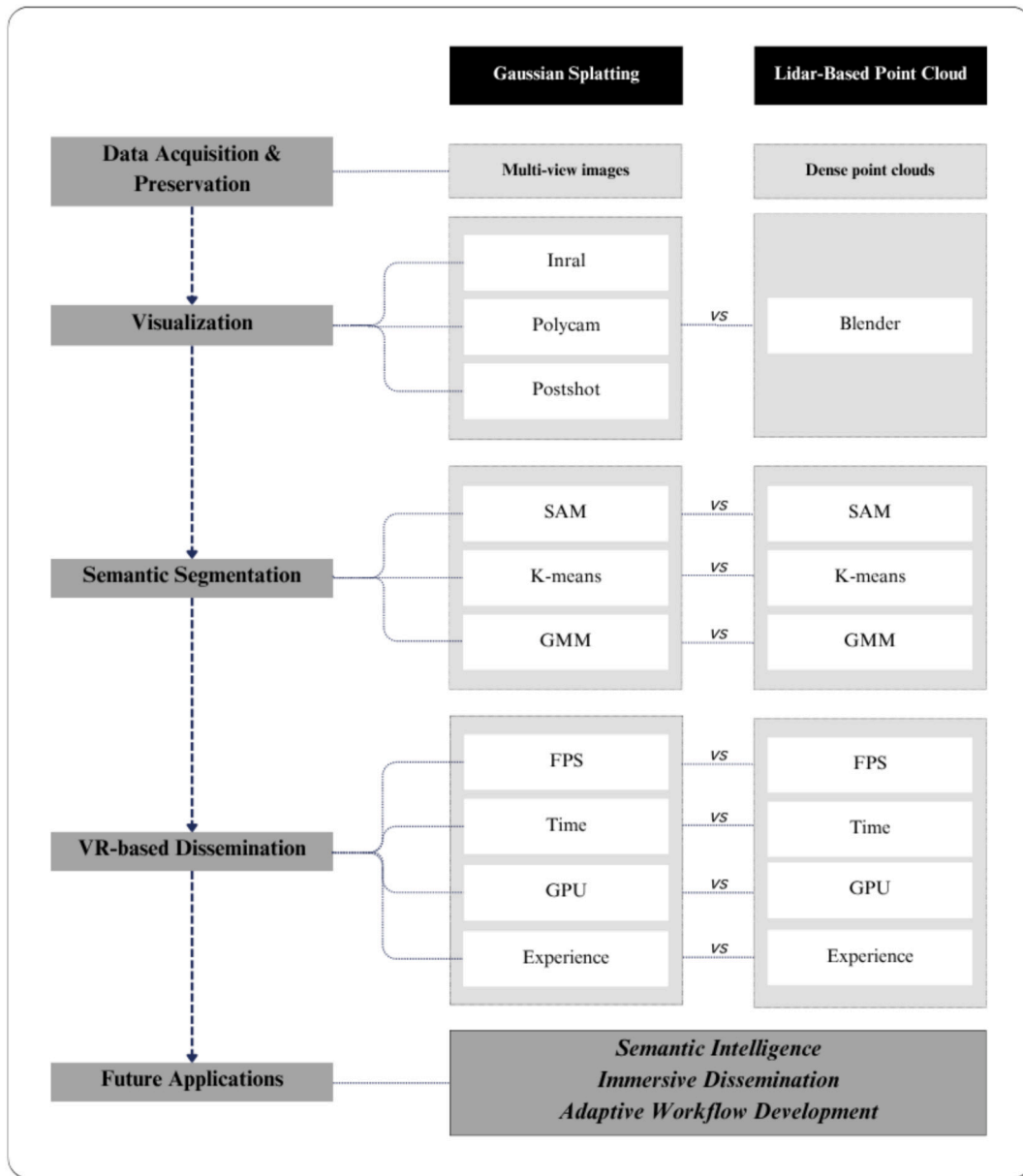


Fig. 2. Workflow-oriented comparison between 3DGS and LiDAR-based point cloud methods.

documentation and long-term digital preservation; visualization is crucial for achieving perceptual fidelity and interpretive clarity; semantic segmentation enables structured information retrieval and facilitates subsequent modeling and management; and VR-based dissemination significantly enhances public accessibility and engagement with digital heritage resources. By systematically comparing the outputs across these critical dimensions, the study aims to clarify each approach's relative strengths and limitations, explicitly define the functional role of 3DGS, and evaluate its practical potential for integration within existing LiDAR-based heritage digitization workflows.

3.1. Case study

This study selects Bouwpub, part of an educational building complex in the Netherlands, as a representative case of modern architectural heritage (Fig. 3). Constructed between 1918 and 1923 in the traditionalist architectural style influenced by the Amsterdam School [68], the building features red brick façades and clearly articulated architectural elements. Its material consistency, standardized construction

methods, uniform materials, and well-documented architectural records, provide a controlled yet representative environment for robustly evaluating and comparing modern 3D digitization techniques. Furthermore, an established HBIM model of Bouwpub, previously constructed from architectural drawings and detailed manual measurements independent of the LiDAR and 3DGS techniques evaluated in this study, offers a precise geometric reference for validation and benchmarking.

3.2. Gaussian splatting-based workflow

To facilitate a clear and structured evaluation, the 3DGS-based workflow is divided into four methodological steps: data collection and preservation, reconstruction and visualization, semantic segmentation, and VR-based dissemination.

3.2.1. Data collection and preservation

Bouwpub's data was collected using multi-view image capture with an iPhone 12 Pro. The choice of a smartphone for data collection was deliberate, motivated by the increasing accessibility of high-quality



Fig. 3. Photographs of Bouwpub.

smartphone imaging capabilities (e.g., built-in LiDAR sensor and advanced computational photography) and the desire to explore low-cost, easily replicable documentation methods suitable for heritage digitization in resource-constrained regions. A total of 124 high-resolution images (3024×4032 pixels) were captured, with overlap consistently exceeding the 70 % recommended threshold by COLMAP, ensuring robust and coherent 3D reconstruction results.

For preservation purposes, original images and processed camera pose data were systematically archived using standardized, open file formats (.jpg images, .csv files for camera poses). Metadata including image acquisition parameters (device type, resolution, timestamps, and camera settings), software processing details (COLMAP and RealityCapture versions), and coordinate system information were documented alongside the datasets. This structured approach ensures long-term data integrity, authenticity, and sustainable reuse for future heritage documentation and comparative research.

3.2.2. 3DGS reconstruction and visualization

To evaluate the practical implementation of 3DGS, this study compares three accessible workflows: (a) Inria Tool, (b) Polycam, and (c) Jawset Postshot. The goal is to identify a representative approach for subsequent comparison with LiDAR-based point cloud visualization (Table 1).

Table 1
Flow of the three visualization methods.

| Approaches | Preprocessing Step | Inputs | Outputs | Notes |
|-----------------|---|---|---|---|
| Inria Tool | COLMAP for camera parameters (txt or .bin) and sparse points (.ply) | Images (from phone & panoramic camera); video frames. | Rendered 3DGS via Inria tool (gaussians. ply) | Must include camera intrinsics and sparse points |
| PolyCam | NA | Images (from phones) | Directly generate 3DGS in the viewer | Easy to use; limited range; close shots improve detail |
| Jawset PostShot | RealityCapture for camera poses (.csv) and sparse point clouds (.ply) | Images (from phone & panoramic camera); video frames. | Refined 3DGS rendering with editable vertex colors (e.g., .exr, .png) | Requires separate export; ensure ASCII and vertex color compatibility |

- Inria Tool⁸ offers a high-fidelity real-time rendering pipeline with full parameter control. Images were first processed using COLMAP to extract camera intrinsics and generate sparse point clouds (cameras.bin, images.bin, and points3D.bin). Training was conducted on a consumer-grade laptop equipped with an NVIDIA RTX 4060 GPU, using a downsampled image resolution of 1512×2016 pixels. Key parameters included 30,000 training steps and a densification threshold of `densify_until_iter = 200,000` to enhance detail in underrepresented regions of the scene.
- Polycam⁹ is a mobile and web-based platform that automates SfM and Gaussian Splatting in the cloud. In this study, 124 high-resolution images (3024×4032 pixels) were captured using an iPhone 12 Pro and uploaded to the Polycam cloud service. The platform automatically generated a 3DGS model with minimal user input, accessible through its built-in viewer.
- Jawset Postshot¹⁰ is a dedicated platform for real-time 3DGS editing and visualization. The workflow began with RealityCapture to extract camera poses (.csv) and sparse point clouds (.ply). In Postshot, training used a low-resolution input (40×40 pixels), 30,000 iterations, and a cap of 3,000,000 splats. The platform supports interactive parameter tuning, vertex color adjustment, and view-dependent rendering optimization.

Overall, Polycam offers an accessible and efficient solution suitable for small-scale scans with minimal technical input. In contrast, the Inria and Postshot workflows demand more preprocessing but provide enhanced flexibility and broader applicability. Table 1 summarizes the technical characteristics of each workflow.

3.2.3. Semantic segmentation

This study adopts three complementary methods to assess the segmentation potential of 3DGS representations in architectural contexts: the **Segment Anything Model (SAM)**, **k-means clustering**, and **Gaussian Mixture Models (GMM)**. These approaches reflect distinct algorithmic paradigms: SAM is a transformer-based model that generates object masks from 2D projections using dense sampling and adaptive confidence thresholds [69]; k-means clusters point-wise features, such as position, color, and scale, into discrete labels based on Euclidean distance [70]; and GMM models the data as a mixture of multivariate Gaussian distributions, optimized through the Expectation-Maximization algorithm [71]. Each method operates on different assumptions regarding data structure and segmentation granularity: SAM favors visual boundaries, k-means assumes uniform compact clusters, and GMM captures overlapping or elliptical regions. This diversity allows a comparative analysis of semantic segmentation performance

⁸ GitHub: <https://github.com/graphdeco-inria/gaussian-splatting>

⁹ Cross-Platform 3D Scanning Floor Plans & Drone Mapping: <https://polycam/>

¹⁰ Jawset Postshot: <https://www.jawset.com/>

under varied architectural features and data representations (Table 2).

- (a) **SAM:** SAM was applied to the 2D projections of the 3DGS model to generate segmentation masks based on visual features [69]. Key parameters included 64 sampling points per side, an IoU threshold of 0.9, and a stability threshold of 0.95, ensuring high-confidence and stable outputs. A single crop layer and a down-scale factor of 2 were used to balance accuracy and computational efficiency. The masks were subsequently projected back onto the 3D model, dividing the facade into ten architectural regions.
- (b) **k-Means:** k-Means was applied to the 3DGS point cloud, using features such as spatial coordinates, RGB values, normals, and Gaussian parameters. The model was clustered into 7 and 14 categories, with semantic labels assigned based on predefined architectural rules (e.g., walls, windows). Results were derived from the optimized 3DGS output.
- (c) **GMM:** GMMs were applied to the 3DGS using spatial, color, and Gaussian-specific attributes. The method assumes that each point belongs to one of k underlying Gaussian clusters and employs the Expectation-Maximization (EM) algorithm to iteratively assign points and optimize cluster parameters. It operates by projecting points into an n -dimensional feature space and adjusting cluster membership and boundaries at each iteration. The segmentation was tested using k values of 7 and 14 to evaluate performance across different levels of granularity.

3.2.4. VR integration and visual dissemination of 3DGS

Unity¹¹ was employed as the VR platform to load and disseminate 3DGS-generated data, enabling evaluation of rendering performance and user experience in immersive environments [72]. The integration of Gaussian Splats into the VR dissemination workflow followed a structured sequence of technical steps, encompassing data preparation, renderer implementation, and environment-specific adaptations.

Table 2

Comparison of SAM, K-Means, and GMM in the context of 3D Gaussian Splatting and point cloud segmentation, focusing on their algorithmic characteristics, data assumptions, and use cases.

| Aspect | SAM | K-Means | GMM |
|------------------------|--|--|---|
| Algorithm Type | Deep Learning (Transformer-based) | Clustering (Centroid-based) | Clustering (Probabilistic model) |
| Learning Type | Supervised / Semi-supervised | Unsupervised | Unsupervised |
| Data Assumptions | Requires large, annotated datasets | Assumes spherical (Euclidean distance) clusters | Assumes data is a mixture of Gaussian distributions |
| Cluster Shape | Irregular, adaptable to object boundaries | Spherical, equal variance clusters | Elliptical, adaptable to varying shapes |
| Output Type | Binary mask or segmented regions | Discrete labels for clusters | Probabilistic assignment to clusters |
| Computation Complexity | High (Requires GPU and large memory) | Low to moderate | Moderate to high |
| Use Cases | Image and video segmentation, object detection | Data clustering, initial segmentation, and preprocessing | Data segmentation, clustering with complex boundaries |

¹¹ Unity: <https://unity.com/cn>

- (a) **Importing Gaussian Splats into the VR scene:** The GaussianSplatRenderer was assigned to a GameObject in Unity, with the corresponding data linked via the GaussianSplatAsset, enabling proper loading and rendering of Gaussian Splats in the VR scene.
- (b) **Transformation alignment with the VR coordinate system:** The position, rotation, and scale of the Gaussian Splats were adjusted to conform to the VR spatial framework, ensuring that the dataset is displayed at a perceptually accurate scale. This alignment is essential for maintaining depth perception, spatial consistency, and user immersion within the VR environment.
- (c) **Interactive operations in VR:** An interactive hotspot system has been implemented in the VR scene to support user engagement and data exploration. Clickable spherical markers were linked to architectural elements, and when selected, they display contextual panels with information such as materials, style, historical background, and function.

3.3. LiDAR-based point clouds workflow

To enable a structured comparison with 3DGS, this study applies the same four methodological steps—data collection and preservation, visualization, semantic segmentation, and VR-based dissemination—to LiDAR-based point clouds.

3.3.1. Data collection and preservation

LiDAR data was collected using the GeoSLAM HORIZON RT,¹² a mobile scanner equipped with an integrated camera. The device enabled Simultaneous Localization and Mapping (SLAM)-based 3D scanning and panoramic image capture, generating dense point clouds in .las format for subsequent processing.

Preservation of LiDAR data involved storing raw and processed point cloud files in standard open formats (.las, .ply). Comprehensive meta-data, including device specifications, scanning parameters (trajectory paths, scanning durations, sensor calibrations), and spatial referencing data (coordinate reference system, alignment transformations), was documented to support the data's long-term authenticity and interoperability. This rigorous preservation strategy facilitates future data reuse, validation, integration into broader digital heritage repositories, and compatibility with existing heritage management platforms.

3.3.2. Visualization

The collected point cloud data was visualized using FARO Connect Viewer,¹³ which supports adjustable rendering modes such as RGB color, intensity, and depth shading. These static rendering modes supported initial data quality assessment, verification, and enhanced spatial interpretation, thus laying the foundation for subsequent real-time dissemination in VR environments.

3.3.3. Semantic segmentation

This subsection explores the application of different segmentation methods to evaluate their effectiveness in extracting architectural features from LiDAR-based point cloud data. Consistent with the approach used for 3DGS, SAM and k-means clustering were applied to the visualized point clouds, while GMMs were utilized for direct segmentation of the raw point cloud data. Due to differences in data characteristics and processing workflows, each method was adapted accordingly.

- (a) **SAM:** When processing point cloud data, SAM leveraged its efficient 2D image segmentation capabilities [73], which were

¹² Geoslam Horizon RT: <https://www.faro.com/zh-CN/Products/Hardware/GeoSLAM-ZEB-Horizon-RT>

¹³ FARO: <https://www.faro.com/en/Products/Software/FARO-Connect-Software>

subsequently projected onto the 3D point cloud using ray casting and nearest-neighbor mapping [74]. To ensure segmentation quality and computational efficiency, the SAM mask generator was configured with a resolution of 64 points per side, an IoU threshold of 0.9, and a stability score threshold of 0.95. Additionally, the segmentation was performed using one crop layer and a downscale factor of 2 to balance detail preservation with processing speed.

- (b) **K-Means:** During the k-Means clustering process, point cloud data was divided into a predefined number of clusters, with 7 or 14 categories applied in this study to ensure effective differentiation of architectural elements. The final clustering results were utilized for automatic semantic segmentation, where certain clusters may correspond to major architectural components such as walls, windows, and roofs.
- (c) **GMM:** For LiDAR-based point clouds, the same GMM approach was applied, using spatial coordinates and intensity values as input features. While the underlying algorithm remained consistent, adaptations were made to account for the sparser structure and lower color information of raw point cloud data. Segmentation was also tested with 7 and 14 clusters.

3.3.4. VR integration and visual dissemination of LiDAR point clouds

The dissemination potential of LiDAR-based point clouds in a VR environment was assessed through data integration and optimized real-time rendering, enabling visual exploration and intuitive navigation.

- (a) **Point cloud format conversion:** Raw point cloud data (.las and .ply) were converted to Unity-compatible formats. The FARO Connect Viewer was used for initial format conversion and refinement, with subsequent export to the .off format via MeshLab, optimized specifically for real-time visualization in Unity.
- (b) **Point cloud rendering and navigation in VR:** The processed datasets were imported and dynamically rendered in Unity using the Point Cloud Viewer plugin, employing adaptive point-size scaling and occlusion culling techniques. This facilitated real-time interactive navigation, allowing users to dynamically explore and visually inspect the heritage dataset from various angles within an immersive VR context.

3.4. Comparative analysis

The comparative analysis of 3DGS and LiDAR-based point clouds is structured around three dimensions—visualization quality, semantic segmentation accuracy, and visual dissemination capability in VR. This comparative framework is specifically designed to uncover the complementary strengths of each method, thus guiding their potential integration into an optimized workflow for digitizing modern architectural heritage.

3.4.1. Visualization quality

Evaluated via Laplacian Variance scores, emphasizing visual clarity

and detail preservation. Results aim to inform how visual realism from 3DGS could be integrated with the structural accuracy of LiDAR.

3.4.2. Semantic segmentation accuracy

Precision and recall metrics calculated against an independently created HBIM model as geometric reference, guiding potential semantic data integration strategies (Fig. 4).

3.4.3. Visual dissemination in VR

Assessment of real-time rendering performance and user navigation responsiveness, aiming to identify integrated visualization pathways combining efficient rendering of 3DGS with detailed structure provided by LiDAR.

4. Results

This section presents comparative results between 3DGS and LiDAR-based point cloud methods. The analysis is organized by evaluation criteria: visualization quality, semantic segmentation accuracy, and visual dissemination performance in VR environments.

4.1. Data collection and preservation

Regarding data acquisition and preservation, notable differences emerged between the two methodologies. The 3DGS workflow demonstrated high accessibility, leveraging consumer-grade smartphones for image capture, thus significantly lowering documentation costs and technical barriers. However, its reliance on image quality and controlled acquisition conditions introduces risks to data consistency and long-term authenticity. Conversely, LiDAR-based scanning provided robust and accurate geometric documentation, offering greater data authenticity and integrity due to standardized acquisition practices and mature preservation protocols (e.g., las and ply formats). Despite these strengths, LiDAR workflows typically entail higher operational complexity, resource demands, and storage requirements. These contrasts underscore the complementary nature of the two methods, reinforcing the value of hybrid digitization strategies to balance preservation quality, data accessibility, and cost efficiency in heritage digitization projects.

4.2. Visualization quality comparison

To evaluate visualization quality, representative results for both 3DGS and LiDAR-based point clouds were generated and compared using qualitative visual assessment and quantitative Laplacian Variance metrics.

For the 3DGS, three implementations were initially examined. The Inria tool provided reconstructions with high geometric clarity and distinct architectural features, particularly evident in façade details (Fig. 5a). Polycam demonstrated balanced geometric and textural accuracy through its automated, cloud-based optimization (Fig. 5b). Postshot, although limited by lower resolution, delivered appealing



Fig. 4. HBIM / HBIM with point cloud.

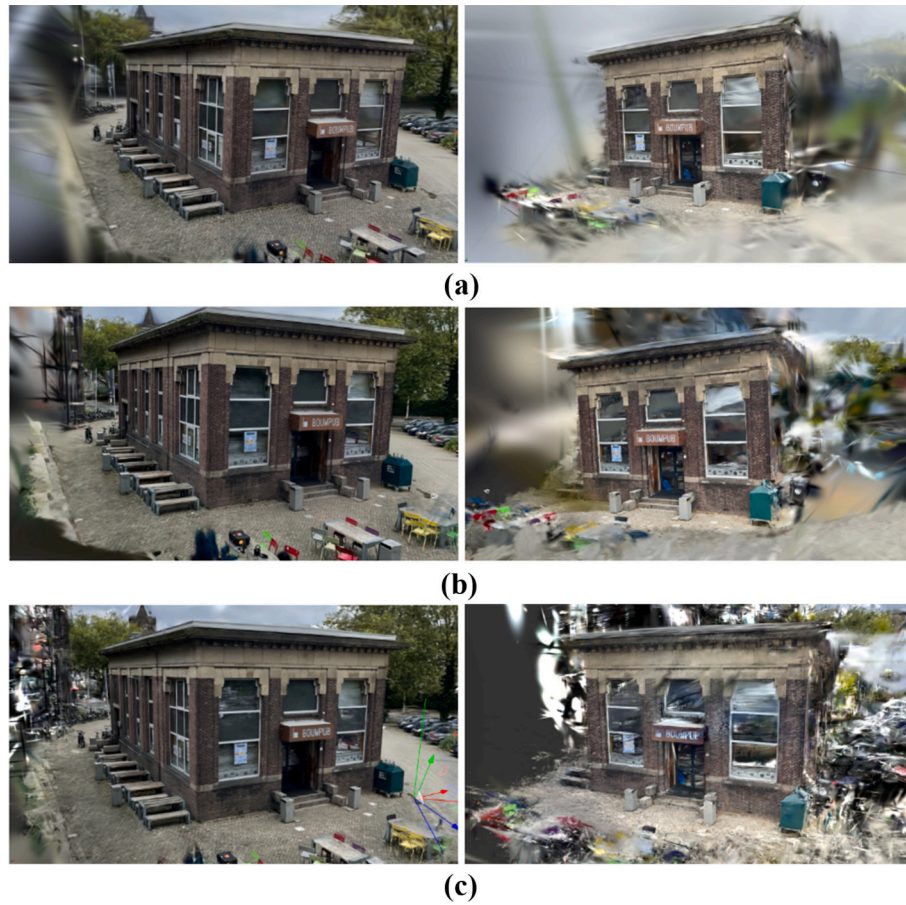


Fig. 5. Visualization results using (a) Inria tool, (b) Polycam, and (c) Postshot.

visuals with rich colors and minimal artifacts due to real-time adaptive shading (Fig. 5c). Among these, the Polycam-generated 3DGS model was selected as the representative dataset for subsequent quantitative comparison due to its balance of visual fidelity, detail preservation, and practical usability in heritage digitization contexts.

The LiDAR-based point cloud generated by GeoSLAM presented a dense, spatially coherent geometric representation of the building façade, effectively capturing structural elements such as walls, openings, and rooflines, despite limited fine-scale textural details (Fig. 6a). The accompanying panoramic images supported spatial interpretation and contextualization (Fig. 6b).

The quantitative comparison utilized Laplacian filtering (Fig. 7). The resulting Laplacian Variance scores indicated that the Polycam-based 3DGS model (2021.88) retained significantly sharper visual details

and higher-frequency information than the LiDAR-based point cloud (1181.53). The HBIM ground-truth model, used as a geometric reference, yielded the highest score (3493.74), reflecting its inherent structural completeness. These findings suggest that the 3DGS approach (represented by Polycam) is better suited than LiDAR for visualization tasks that demand high-resolution clarity and precise detail preservation.

4.3. Semantic segmentation accuracy comparison

Qualitative assessment revealed clear differences in semantic segmentation quality between the 3DGS and LiDAR-based datasets.

For the **3DGS model** (generated by Polycam; Fig. 8), the SAM method (Fig. 8a) exhibited irregular boundaries and notable

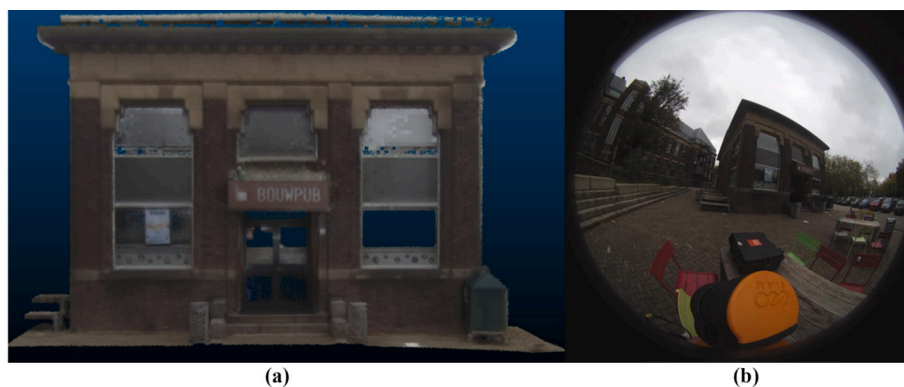


Fig. 6. Visualization results of LiDAR-based point clouds: (a) Point cloud of Bouwpub's front-face and (b) Panoramic photo from GeoSLAM.

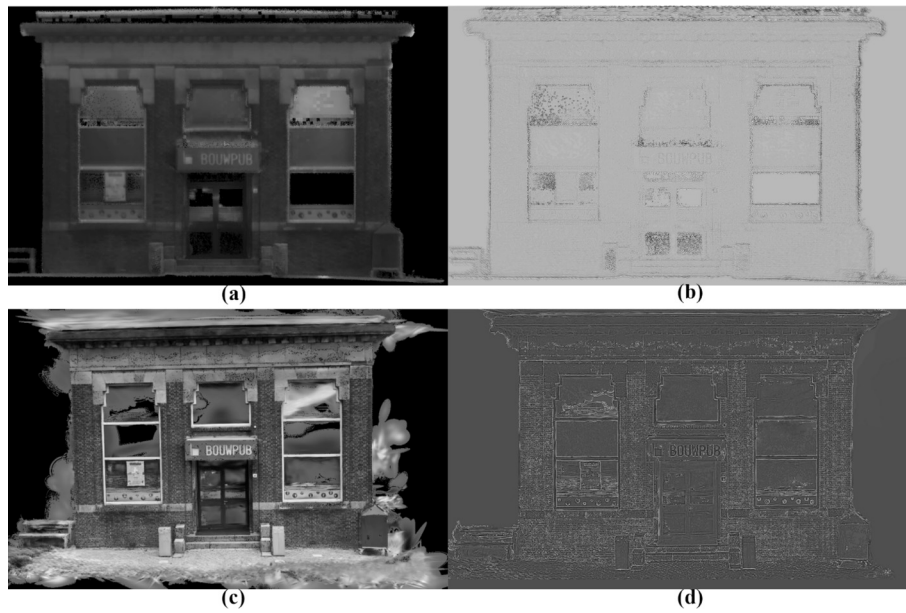


Fig. 7. Images of Laplacian filter's results: (a) Image of GeoSLAM point cloud in Greyscale; (b) Laplacian filter applied to GeoSLAM Point Cloud; (c) Image of Gaussian splatted point cloud in Greyscale; (d) Laplacian filter applied to Image of Gaussian splatted point cloud.

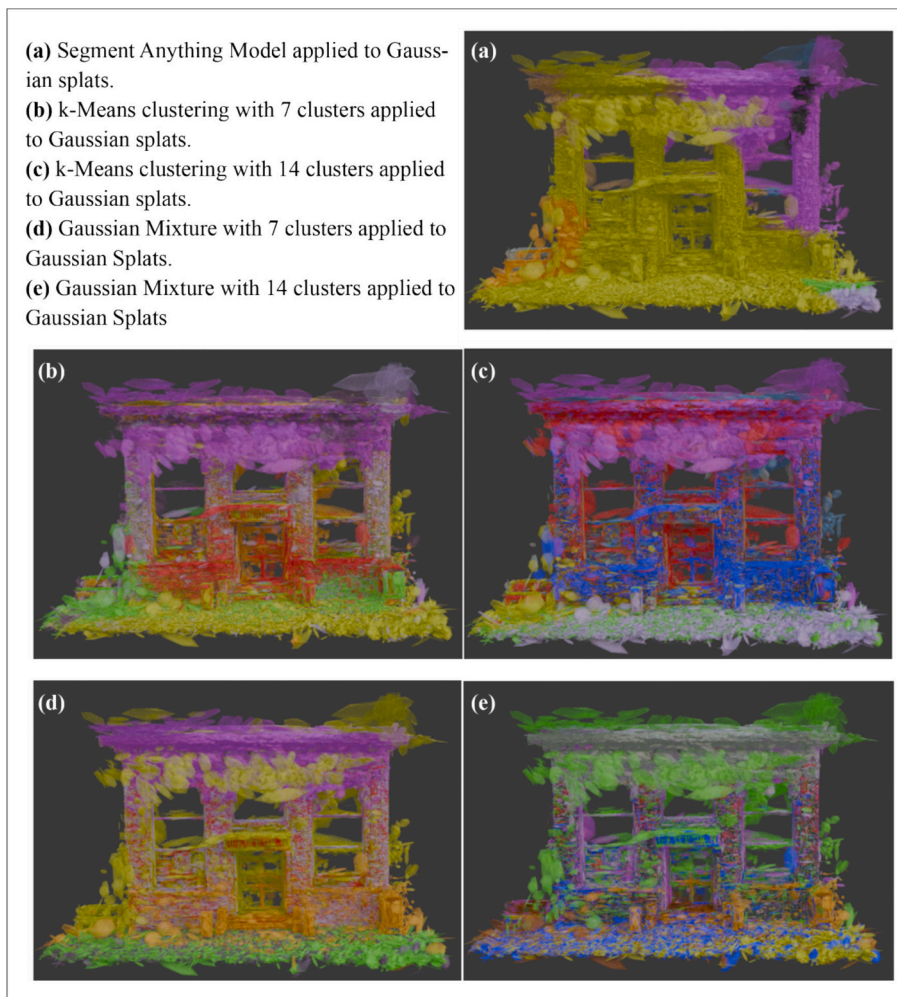


Fig. 8. Segmented Gaussian splatted point cloud results.

misalignment with actual architectural elements due primarily to sparse point distributions and projection distortions. K-means clustering (Fig. 8b, Fig. 8c; $k = 7, 14$) moderately improved segmentation clarity but still lacked distinct differentiation of detailed components. The GMM method (Fig. 8d, Fig. 8e; $k = 7, 14$) produced the most consistent and visually coherent segmentation results, clearly separating major volumes like roofs and ground areas despite ongoing challenges with smaller details such as windows and canopies. Thus, **GMM ($k = 14$)** was selected as the most representative 3DGS segmentation approach for subsequent quantitative accuracy comparisons.

For the **LiDAR-based point cloud** dataset (Fig. 9), SAM segmentation (Fig. 9a) successfully isolated primary architectural components such as walls, roofs, and doors, despite occasional local inaccuracies due to occlusions. K-means segmentation (Fig. 9b, Fig. 9c; $k = 7, 14$) was comparatively coarse at lower resolutions but moderately improved at higher resolutions, although it remained fragmented in certain areas. GMM segmentation (Fig. 9d, Fig. 9e; $k = 7, 14$) provided clear and detailed separation at higher resolutions, effectively delineating roofs, walls, and doors. Nevertheless, the **SAM approach** stood out due to its clearer overall segmentation structure and better correspondence with architectural boundaries. Consequently, **SAM** was chosen as the representative LiDAR segmentation method for quantitative comparison.

Quantitative comparison between the selected segmentation methods (GMM for 3DGS and SAM for LiDAR) using precision and recall metrics further clarified their respective strengths (Fig. 10). The precision heatmap (Fig. 10a) indicates that LiDAR-based SAM segmentation precision varied significantly (approximately 10 %–77 %), achieving high accuracy for major elements (walls, roofs) but lower accuracy for complex elements (canopies) due to structural complexity and limited point coverage. The recall heatmap (Fig. 10b) revealed consistently

higher recall values for LiDAR-based SAM segmentation, particularly for walls and stairs, attributable to the denser point distribution enabling more comprehensive segmentation coverage. In contrast, the 3DGS GMM segmentation demonstrated relatively lower recall values, especially for components with fewer points, such as canopies, limiting detection accuracy.

The bar plot summarizing mean precision and recall (Fig. 10c) explicitly illustrates these distinctions, highlighting that LiDAR-based SAM segmentation generally achieves superior recall, better suited to applications demanding comprehensive segmentation of architectural features. Conversely, 3DGS-based GMM segmentation exhibited consistently stable precision but at the cost of completeness. Overall, these results suggest that LiDAR (with SAM) provides superior segmentation completeness, advantageous for detailed heritage documentation, whereas 3DGS (with GMM) offers consistent segmentation precision better suited to scenarios prioritizing segmentation stability and visual coherence.

4.4. Visual dissemination performance in VR comparison

To evaluate visual dissemination capabilities in VR (Unity), both 3DGS and LiDAR-based point cloud models were first qualitatively assessed and followed by a detailed quantitative comparison of rendering performance and responsiveness metrics.

3DGS provided visually consistent and realistic models characterized by smooth, continuous textures and effective color blending, significantly enhancing immersive realism and spatial clarity. Despite minor visual artifacts in highly detailed regions (e.g., windows), overall visual quality was maintained at a high level (Fig. 11).

LiDAR-based point clouds delivered detailed geometric

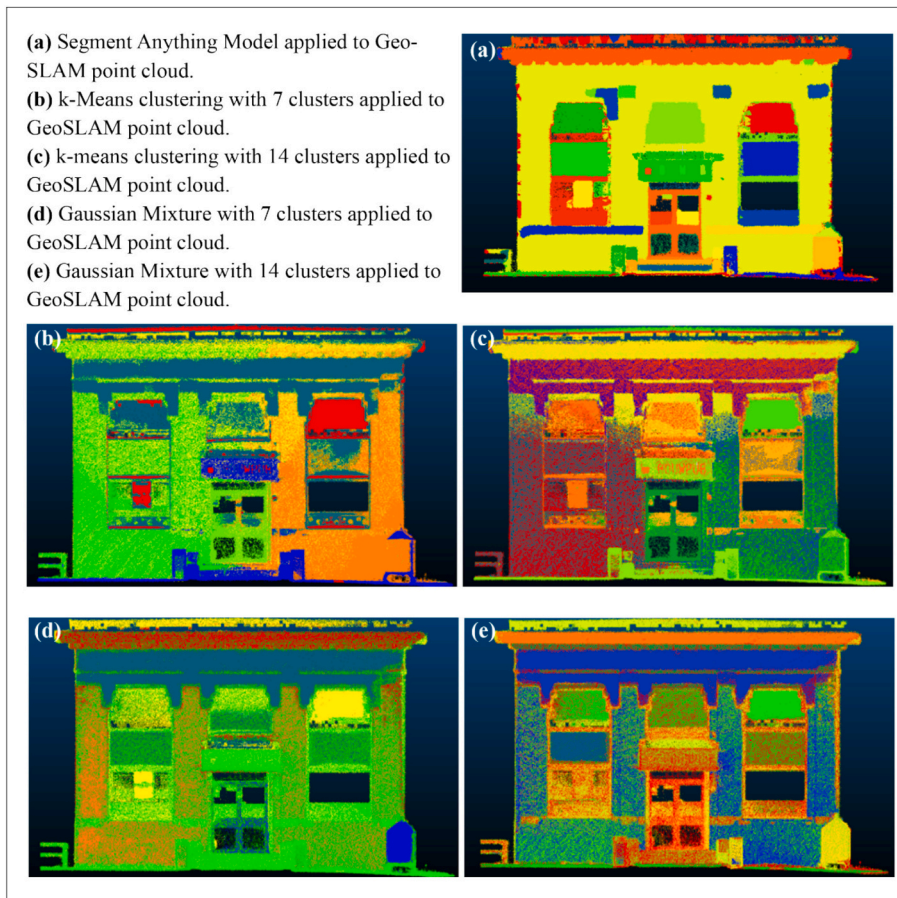


Fig. 9. Segmented GeoSLAM point cloud results.

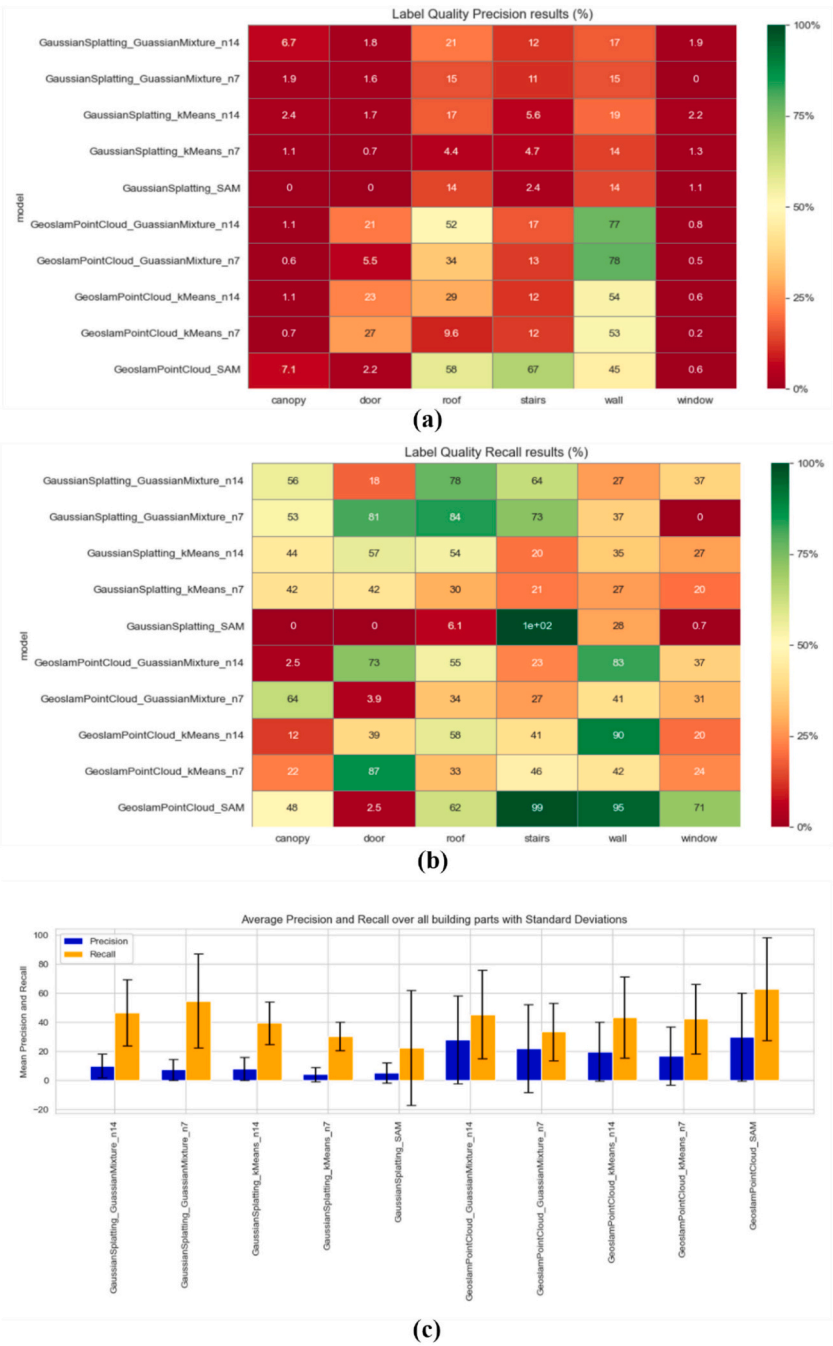


Fig. 10. Precision and recall across different methods: (a) Heat map for precision scores on all methods; (b) Heat map for recall scores on all methods; (c) Bar plot with mean precision and recall with error bars on all methods.



Fig. 11. 3DGS Visualization and interactive operation in Unity.

representations with accurate spatial structures. However, visual fragmentation, transparency issues, and noticeable gaps detracted from visual realism and immersive experience. User interaction was also perceptibly hindered by visual discontinuities and slower responses (Fig. 12).

A direct quantitative comparison (Table 3) strongly emphasized the performance gap between the two methods. Specifically, the 3DGS model consistently outperformed LiDAR-based visualization with significantly higher real-time rendering stability (3DGS: 60–90 FPS vs. LiDAR: 15–60 FPS), markedly reduced GPU load (3DGS: 12–25 % vs. LiDAR: 35–55 %), dramatically lower memory consumption (3DGS: 13.6 MB vs. LiDAR: 562 MB), and substantially lower interaction latency (3DGS: <10 ms vs. LiDAR: ~35 ms). These substantial differences confirm that 3DGS excels not only in visual coherence and immersive quality but also in scalability, responsiveness, and computational efficiency. Conversely, despite its strengths in geometric accuracy, the LiDAR method's limitations in rendering efficiency, latency, and immersive consistency present notable challenges for effective VR-based dissemination. The observed complementarity between 3DGS, offering superior visual dissemination, and LiDAR, providing robust geometric completeness, highlights promising opportunities for methodological integration. The empirical findings presented in this study further validate the practical feasibility and benefits of such an integrated approach, laying a foundation for developing optimized hybrid solutions in immersive architectural heritage digitization.

5. Discussion

The comparative results clearly indicate that 3DGS and LiDAR-based point clouds possess complementary rather than competing strengths. While 3DGS offers intrinsic advantages in visual quality, photorealism, and VR-based dissemination, making it highly effective for immersive public engagement, LiDAR excels in geometric accuracy, semantic completeness, and structural documentation, essential for rigorous heritage analysis and professional archiving. These distinct methodological strengths suggest that neither method alone fully addresses the complex requirements of digital heritage practices. Therefore, integrating the visual and dissemination advantages of 3DGS with the structural and semantic accuracy of LiDAR could lead to an optimal, hybrid digitization workflow. The following sections explore specific integration strategies, potential applications, and methodological advancements based on this complementary relationship.

5.1. Integration of 3DGS and LiDAR-based point clouds

Based on the comparison, 3DGS has shown remarkable performance

Table 3

Dissemination comparison between 3DGS and LiDAR point clouds in VR.

| Aspect | Point Cloud | 3DGS |
|-----------------------------|------------------------------------|--|
| Rendering Performance | High computational cost | Optimized for real-time VR |
| Loading Time | 40s (13 million vertices) | 1 s |
| Real-Time FPS | 15–60 (requires LoD) | 60–90 |
| Memory Usage | 562 MB | 13.6 MB |
| GPU Processing Overhead | 35–55 % | 12–25 % |
| Visual Clarity & Depth | Missing parts and transparency | More continuous and realistic |
| Latency | ~35 ms | ~10 ms |
| Texture Representation | Dependent on point density | Smooth texture appearance |
| Depth Perception | Depth perception challenges | More stable and solid perception |
| Transparency Handling | Floating artifacts cause confusion | Better, but still has transparency artifacts |
| Interaction Precision | Lower accuracy | More precise and reliable |
| Object Selection Accuracy | Easy to select | Easy to select |
| Immersion & User Experience | Less immersive | Highly immersive |
| Realism and Immersion | Limited due to artifacts | Realistic due to blended textures |

in image-based 3D reconstruction; its role within LiDAR-dominant workflows for heritage documentation remains underexplored. Rather than viewing 3DGS as a competing acquisition method, this study proposes repositioning it as a post-processing visualization and dissemination layer. In point cloud-based workflows, where geometric accuracy is paramount, 3DGS can serve as a rendering enhancement mechanism, improving visual coherence, real-time performance, and user dissemination in immersive environments. To enable such integration, two strategies are proposed: one based on structured image rendering using Blender, and the other on point cloud subsampling combined with Level-of-Detail (LOD) rendering.

5.1.1. Blender-based rendering of dense point clouds for 3DGS integration

A Blender-based rendering pipeline was developed to circumvent the computational limitations of direct point cloud-to-3DGS conversion. This method imports denoised and optimized LiDAR point clouds into Blender, where the original camera trajectory is reconstructed via Python scripting. A cube-map image capture setup is created by placing six virtual cameras at each position using the “Camera Array Tool for Blender.” This setup ensures systematic, multi-angle rendering of the entire structure (Fig. 13).

The generated image dataset—typically exceeding 1800



Fig. 12. Dense point cloud visualization in unity.



Fig. 13. Blender-Based Integration of Point Clouds and 3D Gaussian Splatting. (a) Overview of the 3D Reconstruction in Blender; (b) Result of Blender-Based splatting.

views—serves as input to the COLMAP and Postshot pipeline for Gaussian Splatting reconstruction. Since the images are rendered from the point cloud, this approach avoids registration inconsistencies between real-world photos and spatial data. The resulting 3DGS model preserves both the structural integrity of the original point cloud and the visual continuity required for immersive visualization. Fully compatible with game engines such as Unity and Unreal Engine, the output supports real-time rendering and dissemination applications, offering a scalable and resource-efficient solution for transforming large-scale heritage datasets into lightweight, high-quality models.

5.1.2. Subsampled point cloud reconstruction with LOD-enhanced 3DGS

A second strategy involves generating a 3DGS model from LiDAR-derived point clouds strategically subsampled and aligned with photogrammetric inputs. The process begins with SfM reconstruction using high-resolution images, producing a sparse point cloud and camera poses. The LiDAR data is then cropped, denoised, and downsampled to retain the primary architectural features while reducing data volume.

The LiDAR dataset is registered to the SfM coordinate system to ensure spatial consistency, enabling accurate alignment of geometric and photometric data (Fig. 14).

This hybrid dataset is subsequently used to generate Gaussian Splats, with the addition of LOD techniques to manage rendering complexity adaptively. LOD3DGS dynamically adjusts the level of detail based on viewer distance, improving runtime performance while preserving visual fidelity. Although LOD-based splatting has been demonstrated in controlled indoor environments, this study represents an early attempt to scale the method to architectural heritage scenarios. The approach combines LiDAR's geometric accuracy with 3DGS's rendering efficiency, supporting high-performance deployment in immersive VR applications.

5.1.3. Summary of the two integration methods

Blender-based multi-angle rendering and LOD-enhanced subsampled reconstruction demonstrate distinct yet complementary approaches to embedding 3DGS within LiDAR-based workflows. The Blender method

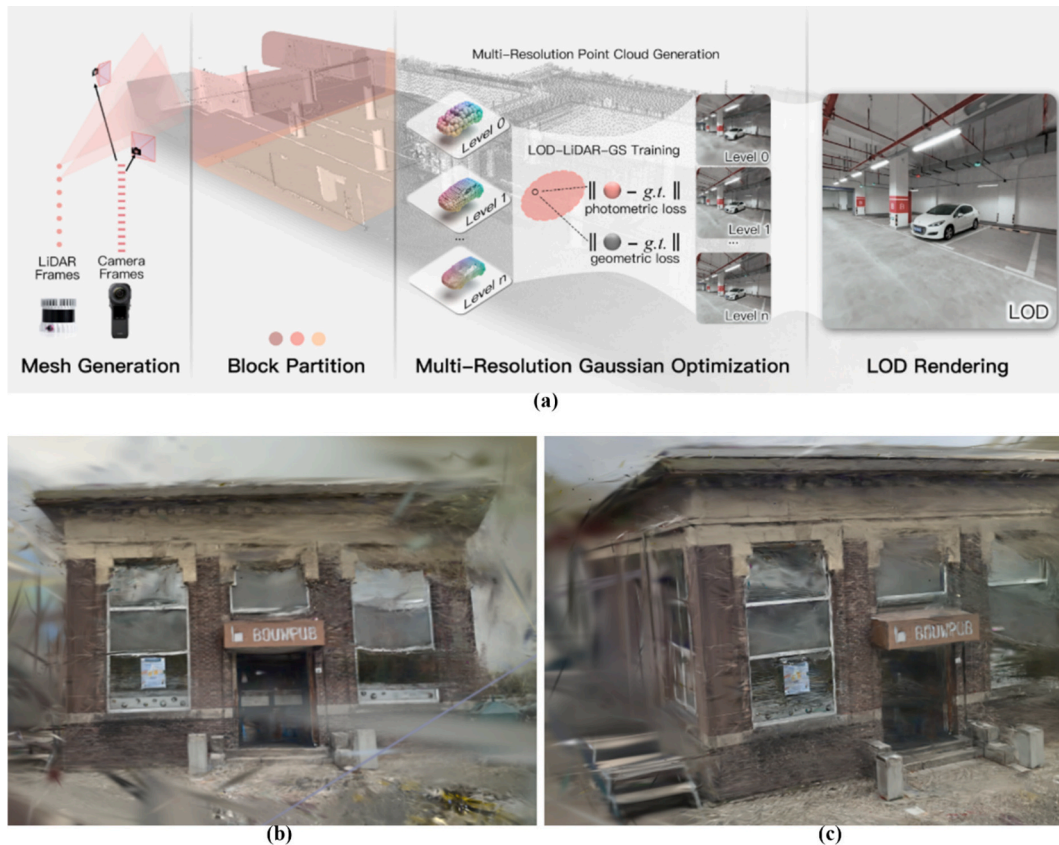


Fig. 14. (a) LOD3DGS Workflow [75] and (b), (c) LiDAR Points & Images Results.

is ideal for dense point clouds lacking high-quality imagery, enabling consistent splatting results through synthetic, geometry-aligned images. In contrast, the LOD3DGS approach suits hybrid datasets where LiDAR and photogrammetry can be jointly processed, supporting scalable rendering with adaptive resolution control. Despite their differences, both approaches assign 3DGS a shared role: a visualization abstraction layer. Rather than replacing LiDAR's role in precise geometric capture, 3DGS enhances surface continuity, dissemination, and real-time performance, particularly in immersive applications. LiDAR provides spatial accuracy in this modular structure, image-based inputs supply texture fidelity, and 3DGS delivers an accessible, cohesive output for visualization and engagement.

These integration strategies highlight the complementary strengths of LiDAR and 3DGS. While LiDAR ensures spatial accuracy and supports semantic modeling, 3DGS enhances real-time responsiveness and immersive visualization. Together, they form a dual-layered framework: a geometric core underpinned by LiDAR [40,42], and an expressive surface enabled by Gaussian rendering [31–33]. This structure supports both analytical precision and visual engagement, fulfilling the technical and communicative goals of heritage digitization.

5.2. Extended potential of 3D Gaussian splatting in heritage workflows

As clarified in the previous sections, 3DGS demonstrates substantial potential as a visualization and dissemination layer within LiDAR-based heritage workflows. Looking forward, 3DGS is poised to extend its role beyond technical integration, offering transformative possibilities for heritage segmentation, immersive dissemination and adaptive workflow development. These future applications align with the third sub-objective of this research: to explore how 3DGS can enhance existing digitization practices in terms of both efficiency and expressiveness. The following discussion outlines three potential directions for 3DGS in modern architectural heritage workflows.

5.2.1. Semantic intelligence: Automated segmentation and HBIM-enriched representation

One of the most promising future applications of 3DGS lies in automated semantic segmentation and semantic enrichment. While traditional point cloud methods have already been employed to extract meaningful architectural elements through machine learning, 3DGS introduces a novel representational structure—layered Gaussian primitives—that supports refined object boundaries and high-frequency detail. This characteristic opens the door for integrating deep learning-based classifiers specifically tailored for architectural typologies, enabling high-precision recognition of walls, windows, cornices, and other elements.

In particular, coupling 3DGS with HBIM offers a powerful pathway for semantic structuring. Gaussian splats can serve as an intermediary visualization layer bridging raw spatial data and parametric HBIM elements, especially when enhanced through semantic labeling algorithms [57,58]. Furthermore, the expressiveness of 3DGS allows metadata such as material conditions and intervention histories to be attached as interactive overlays, supporting multidimensional interpretation of architectural features.

As an initial exploration into semantic enrichment and integrated visualization, our team has developed a preliminary web-based platform that combines semantic HBIM data, detailed LiDAR point clouds, and Gaussian splatting for interactive, multilayered heritage presentation. In this implementation, Gaussian splatting provides an intuitive photorealistic visualization layer, beneficial for public engagement and general comprehension of heritage sites. The HBIM semantic layer enriches the model with structured information on architectural components, historical contexts, and materials, thus facilitating professional analysis and educational outreach. Concurrently, the LiDAR-derived point cloud ensures precise geometric accuracy, supporting heritage managers with detailed structural information crucial for accurate condition

assessments and conservation strategies. Early user tests have indicated promising outcomes in interpretability, user engagement, and professional utility, underscoring the effectiveness of this integrated semantic-visual framework. Detailed evaluation, including comprehensive technical workflows and quantitative analyses, will be presented in a future dedicated publication.

5.2.2. Immersive interaction: Enhancing heritage exploration in VR/AR

3DGS is uniquely suited to support immersive exploration of architectural heritage in VR/AR environments, because 3DGS enables photorealistic, smooth-surface rendering optimized for real-time interaction [31–33]. In educational and curatorial contexts, this supports more intuitive spatial perception and allows non-expert audiences to navigate complex architectural environments.

Future applications may include interactive storytelling platforms in VR, where users explore a building and activate information nodes embedded within the Gaussian representation, such as material annotations, historical narratives, or comparisons across time periods. Real-time overlays of conservation data or structural assessments could also be enabled within the 3DGS environment, supporting professional workflows. Moreover, by incorporating LOD3DGS into web-based platforms, lightweight yet detailed models could be deployed online for collaborative access, making digital heritage more scalable and participatory. A notable innovation in our prototype is the seamless integration of Gaussian splats with dynamic interactive hotspots, providing a visually coherent and contextually responsive exploration experience. Initial trials conducted at selected historical buildings demonstrated a significant enhancement in participants' ability to comprehend spatial layouts, identify heritage elements, and engage meaningfully with conservation narratives.

Future applications may further include integrating real-time overlays of conservation data or structural assessments directly within 3DGS environments. Additionally, incorporating LOD3DGS into web-based platforms could enable lightweight yet detailed models for broader collaborative access.

5.2.3. Workflow evolution: Designing future pipelines with 3DGS integration

Beyond use-specific advancements, 3DGS offers substantial potential for reshaping broader digital heritage workflows. Rather than merely serving as an endpoint for visualization, 3DGS can function as a dynamic node within interoperable heritage documentation pipelines. Outputs from point cloud segmentation or HBIM modeling could be visually rendered via 3DGS, enabling streamlined communication among conservationists, architects, historians, and the general public. This capability positions 3DGS as both a visual and interactive module within comprehensive heritage information systems.

As part of our ongoing research, a structured hybrid data acquisition and processing workflow has been preliminarily established and tested. UAV photogrammetry was employed for documenting elevated or inaccessible architectural features, such as domes, towers, and complex rooftops, resulting in textured Gaussian Splats with high visual fidelity. Concurrently, TLS was used to capture accurate geometric data of façades, interiors, and ground-level details. Our initial practical implementations have successfully demonstrated effective spatial alignment and integration of these datasets, generating coherent 3D digital twins that combine precise LiDAR geometry with detailed Gaussian-based visualization.

Early testing in real-world heritage scenarios has highlighted notable benefits in collaborative stakeholder engagement, enabling both expert groups and non-technical audiences to interact intuitively with complex data. Preliminary feedback indicated significant improvements in communication efficiency between conservation specialists, architects, and site managers, streamlining conservation planning and decision-making processes.

This integrated workflow aligns closely with the vision promoted by

the AHII, advocating interoperable, semantically enriched, and visually intelligible heritage data frameworks. In our implemented multi-layered architecture, LiDAR provides the foundational geometric accuracy, HBIM delivers structured semantic and parametric information, and 3DGS operates as the primary interface for visualization, public engagement, and professional interaction. This modular framework supports scalable dissemination via Web3D platforms or immersive VR environments, encouraging multi-disciplinary collaboration and efficient reuse of heritage data.

Moving forward, future research should further refine data fusion methodologies, optimize Gaussian-based visualization modules for larger-scale deployments, and establish standard protocols for embedding 3DGS seamlessly within AHII-compatible workflows. Comprehensive technical details, precise workflow evaluations, and case-specific quantitative results from our ongoing projects will be systematically presented in dedicated future publications.

5.3. Limitations and outlook

While this study demonstrates the feasibility and value of integrating 3DGS with LiDAR for modern architectural heritage digitization, several limitations should be acknowledged. These relate primarily to data dependency, computational performance, workflow maturity, and cross-platform interoperability.

One notable limitation is 3DGS's reliance on high-quality image input. Accurate reconstruction depends on well-calibrated, high-resolution photographs with consistent lighting and full surface coverage. In this study, while the available imagery was sufficient for methodological validation, issues such as exposure variation and partial occlusion may have introduced localized errors in depth estimation and texture fidelity [76,77]. These constraints underscore the importance of refined image acquisition protocols rather than reflecting inherent weaknesses in the 3DGS technique. A second limitation concerns hardware constraints. Due to the high GPU demand associated with converting dense LiDAR point clouds into Gaussian splats [78], this study adopted alternative integration strategies, such as Blender-based image rendering and LOD3DGS pipelines, to maintain feasibility. These workarounds introduced trade-offs in model resolution and processing granularity. Finally, the integration of 3DGS into structured digital heritage workflows, such as HBIM and the AHII, remains at an early stage. Currently, 3DGS lacks standardized compatibility with GIS-based spatial data formats, parametric modeling platforms, and semantic conservation datasets. This limits its interoperability within long-term heritage management systems. Developing shared protocols for 3DGS–LiDAR–HBIM data exchange and embedding visualization components into existing workflows should be a priority for future research.

Despite these limitations, the study contributes a practical roadmap for integrating 3DGS into LiDAR-dominant heritage workflows, supported by two viable technical strategies. Moving forward, research should focus on three fronts: (a) improving image acquisition pipelines for greater reconstruction accuracy, (b) optimizing computational performance through multi-resolution or hardware-specific methods, and (c) formalizing standardized integration pathways for embedding 3DGS into broader heritage information infrastructures.

6. Conclusion

This paper presented the application of 3DGS within the domain of modern architectural heritage digitization and evaluated its integration with LiDAR-based workflows. Addressing the identified research gaps, the study fulfilled three primary objectives: (a) empirically assessed the feasibility of 3DGS in real-world heritage scenarios, (b) clarified its functional role within LiDAR-dominated digitization pipelines, and (c) explored integration strategies that enhanced both the efficiency and expressiveness of heritage documentation.

The comparative analysis confirmed that 3DGS excelled in

photorealistic rendering and VR-based dissemination, offering light-weight and immersive outputs. However, it remained limited by its reliance on high-quality image inputs and reduced geometric precision in complex or occluded areas. In contrast, LiDAR ensured spatial accuracy and segmentation reliability, albeit with higher computational costs and lower visual engagement. These complementary characteristics justified the development of hybrid workflows. Two integration strategies, Blender-based multi-angle rendering and LOD3DGS, demonstrated how 3DGS could serve as a visualization and dissemination layer built upon LiDAR-acquired geometry.

While promising, further work is needed to strengthen 3DGS's interoperability within broader heritage infrastructures. Future research should focus on improving image-based data acquisition, standardizing workflows that integrate 3DGS with HBIM and LiDAR, ensuring data interoperability with geospatial management platforms (e.g., GIS) and heritage documentation databases (e.g., Docomomo), and advancing LOD3DGS for web-based visualization.

CRedit authorship contribution statement

Yingwen Yu: Writing – original draft, Visualization, Methodology, Investigation, Formal analysis, Conceptualization. **Edward Verbree:** Writing – review & editing, Supervision, Conceptualization. **Peter van Oosterom:** Writing – review & editing, Supervision, Formal analysis. **Uta Pottgiesser:** Supervision. **Yuyang Peng:** Writing – original draft, Methodology, Formal analysis. **Florent Poux:** Supervision.

Declaration of competing interest

The authors declare that they have no known competing financial interests or personal relationships that could have appeared to influence the work reported in this paper.

Acknowledgement

This research was conducted as part of the Synthesis Project, and we acknowledge the collective efforts of all team members whose contributions were instrumental in shaping our study. We used AI tools exclusively for improving language clarity and readability.

Data availability

Data will be made available on request.

References

- [1] M.A. Kaptan, A. Ünlü, U. Pottgiesser, Connecting the dots: a global exploration of local Docomomo inventories, *Docomomo J.* 69 (2023) 76–85, <https://doi.org/10.52200/docomomo.69.09>.
- [2] U. Pottgiesser, M. Olweny, K. Manful, O. Uduku, T. Lawson, Shared heritage Africa: a documentary rediscovery, *Mod. Heritage Afr.* (2021) 279, <https://doi.org/10.52200/docomomo.69.ed>.
- [3] S. Labadi, UNESCO, cultural heritage, and outstanding universal value: Value-based analyses of the World Heritage and Intangible Cultural Heritage Conventions, 2013, <https://doi.org/10.5040/9798881809140>.
- [4] B. Qasim Derhem Dammag, D. Jian, A.Q. Dammag, Cultural Heritage Sites Risk Assessment and Management Using a Hybridized Technique Based on GIS and SWOT-AHP in the Ancient City of Ibb, Yemen, *International Journal of Architectural Heritage*, 2025, pp. 1–36, <https://doi.org/10.1080/15583058.2024.2364717>.
- [5] Y. Yu, A.A. Raed, Y. Peng, U. Pottgiesser, E. Verbree, P. van Oosterom, How digital technologies have been applied for architectural heritage risk management: a systemic literature review from 2014 to 2024, *NPJ Heritage Sci.* 13 (1) (2025) 45, <https://doi.org/10.1038/s40494-025-01558-5>.
- [6] M. Li, Disaster risk management of cultural heritage: a global scale analysis of characteristics, multiple hazards, lessons learned from historical disasters, and issues in current DRR measures in world heritage sites, *Int. J. Disast. Risk Reduct.* 110 (2024) 104633, <https://doi.org/10.1016/j.ijdr.2024.104633>.
- [7] G. Aktürk, S.J. Hauser, Integrated understanding of climate change and disaster risk for building resilience of cultural heritage sites, *Nat. Hazards* 121 (4) (2025) 4309–4334, <https://doi.org/10.1007/s11069-024-06970-x>.

- [8] E. Stylianidis, Photogrammetric Survey for the Recording and Documentation of Historic Buildings, Springer, 2020, <https://doi.org/10.1007/978-3-030-47310-5>.
- [9] A.P. Tribhuvan, Preserving our past: a thorough examination of methods and Technologies in Digital Heritage, Int. J. Sci. Technol. 16 (1) (2024), <https://doi.org/10.71097/IJSAT.v16.i1.1324>.
- [10] A. Khalil, S. Stravrovadis, D. Backes, Categorisation of building data in the digital documentation of heritage buildings, Appl. Geomat. 13 (1) (2021) 29–54, <https://doi.org/10.1007/s12518-020-00322-7>.
- [11] J.A. Beraldin, Integration of laser scanning and close-range photogrammetry—The last decade and beyond, in: Proceedings of the XXth ISPRS Congress, 2004, in: <https://www.isprs.org/proceedings/XXXV/congress/comm5/papers/1031.pdf>.
- [12] A.S. Borkowski, A. Kubrat, Integration of laser scanning, digital photogrammetry and BIM technology: a review and case studies, Eng 5 (4) (2024) 2395–2409, <https://doi.org/10.3390/eng5040125>.
- [13] P. Sestras, G. Badea, A.C. Badea, T. Salagean, S. Roşca, S. Kader, et al., Land surveying with UAV photogrammetry and LiDAR for optimal building planning, Autom. Constr. 173 (2025) 106092, <https://doi.org/10.1016/j.autcon.2025.106092>.
- [14] E. Pellis, A. Masiero, M. Betti, G. Tucci, P. Grussenmeyer, A deep learning multiview approach for the semantic segmentation of heritage building point clouds, Int. J. Architect. Heritage (2025) 1–23, <https://doi.org/10.1080/15583058.2025.2485242>.
- [15] Y. Li, L. Zhao, Y. Chen, N. Zhang, H. Fan, Z. Zhang, 3D LiDAR and multi-technology collaboration for preservation of built heritage in China: a review, Int. J. Appl. Earth Obs. Geoinf. 116 (2023) 103156, <https://doi.org/10.1016/j.jag.2022.103156>.
- [16] J. Balado, E. Frías, S.M. González-Collazo, L. Díaz-Vilariño, New trends in laser scanning for cultural heritage, in: D. Bienvenido-Huertas, J. Moyano-Campos (Eds.), New Technologies in Building and Construction: Towards Sustainable Development, Springer Nature Singapore, Singapore, 2022, pp. 167–186, https://doi.org/10.1007/978-981-19-1894-0_10.
- [17] S. Yang, S. Xu, W. Huang, 3D point cloud for cultural heritage: a scientometric survey, Remote Sens 14 (21) (2022), <https://doi.org/10.3390/rs14215542>.
- [18] S. Yang, M. Hou, A. Shaker, S. Li, Modeling and processing of smart point clouds of cultural relics with complex geometries, ISPRS Int. J. Geo Inf. 10 (9) (2021), <https://doi.org/10.3390/ijgi10090617>.
- [19] X. Li, L. Teppati Losè, F. Rinaudo, Documentation for architectural heritage: a historical building information modeling data modeling approach for the Valentino Castle north wing, ISPRS Int. J. Geo Inf. 14 (4) (2025), <https://doi.org/10.3390/ijgi14040139>.
- [20] L. Xu, Y. Xu, Z. Rao, W. Gao, Real-time 3D reconstruction for the conservation of the Great Wall's cultural heritage using depth cameras, Sustainability 16 (16) (2024), <https://doi.org/10.3390/su16167024>.
- [21] S. Dimitriou, O. Kontovourkis, A computational design workflow towards a comprehensive digitization of historic buildings, J. Archaeol. Sci. Rep. 53 (2024) 104319, <https://doi.org/10.1016/j.jasrep.2023.104319>.
- [22] Y. Cao, S. Teruggi, F. Fassi, M. Scaioni, A Comprehensive Understanding of Machine Learning and Deep Learning Methods for 3D Architectural Cultural Heritage Point Cloud Semantic Segmentation. Geomatics for Green and Digital Transition 2022, Springer International Publishing, Cham, 2022, https://doi.org/10.1007/978-3-031-17439-1_24.
- [23] S. Huang, Q. Hu, M. Ai, P. Zhao, J. Li, H. Cui, et al., Weakly supervised 3D point cloud semantic segmentation for architectural heritage using teacher-guided consistency and contrast learning, Autom. Constr. 168 (2024) 105831, <https://doi.org/10.1016/j.autcon.2024.105831>.
- [24] J. Zhao, X. Hua, J. Yang, L. Yin, Z. Liu, X. Wang, A review of point cloud segmentation of architectural cultural heritage, ISPRS Ann. Photogramm. Remote Sens. Spatial. Inform. Sci. X-1/W1-2023 (2023) 247–254, <https://doi.org/10.5194/isprs-annals-X-1-W1-2023-247-2023>.
- [25] J. Moyano, E. N-JJ, M. LL, S. Bruno, Operability of point cloud data in an architectural heritage information model, Int. J. Archit. Herit. 16 (10) (2022) 1588–1607, <https://doi.org/10.1080/15583058.2021.1900951>.
- [26] V.A. Cotella, From 3D point clouds to HBIM: application of artificial intelligence in cultural heritage, Autom. Constr. 152 (2023) 104936, <https://doi.org/10.1016/j.autcon.2023.104936>.
- [27] S. Yang, M. Hou, S. Li, Three-dimensional point cloud semantic segmentation for cultural heritage: a comprehensive review, Remote Sens 15 (3) (2023), <https://doi.org/10.3390/rs15030548>.
- [28] C. Chen, J. Guo, H. Wu, Y. Li, B. Shi, Performance comparison of filtering algorithms for high-density airborne LiDAR point clouds over complex LandScapes, Remote Sens 13 (14) (2021), <https://doi.org/10.3390/rs13142663>.
- [29] H. Zheng, L. Chen, H. Hu, Y. Wang, Y. Wei, Research on the digital preservation of architectural heritage based on virtual reality technology, Buildings 14 (5) (2024), <https://doi.org/10.3390/buildings14051436>.
- [30] B. Kerbl, G. Kopanas, T. Leimkühler, G. Drettakis, 3d gaussian splatting for real-time radiance field rendering, ACM Trans. Graph. (2023) 139, 1–14, <https://doi.org/10.1145/3592433>.
- [31] Y. Zhang, G. Jiang, M. Li, G. Feng, The 3D Gaussian splatting SLAM system for dynamic scenes based on LiDAR point clouds and vision fusion, Appl. Sci. 15 (8) (2025), <https://doi.org/10.3390/app15084190>.
- [32] C. Yan, D. Qu, D. Xu, B. Zhao, Z. Wang, D. Wang, et al., Gs-slam: Dense visual slam with 3d gaussian splatting, in: Proceedings of the IEEE/CVF Conference on Computer Vision and Pattern Recognition, 2024, <https://doi.org/10.1109/CVPR52733.2024.01853>.
- [33] M. Li, S. Liu, H. Zhou, G. Zhu, N. Cheng, T. Deng, et al., Sgs-slam: Semantic gaussian splatting for neural dense slam, in: European Conference on Computer Vision, Springer, 2024, https://doi.org/10.1007/978-3-031-72751-1_10.
- [34] W. Wang, Editor real-time fast 3D reconstruction of heritage buildings based on 3D Gaussian splashing, in: 2024 IEEE 2nd International Conference on Sensors 2024, Electronics and Computer Engineering (ICSECE), Aug. 2024, pp. 29–31, <https://doi.org/10.1109/ICSECE61636.2024.10729491>.
- [35] E. Cieslik, 3D Digitization in Cultural Heritage Institutions Guidebook, Available from: https://www.academia.edu/68906660/3D_Digitization_in_Cultural_Heritage_Institutions_Guidebook2020.
- [36] A. Prokop, P. Nazarko, L. Ziemiański, Digitalization of historic buildings using modern technologies and tools, Budownictwo i Architektura. 20 (2) (2021), <https://doi.org/10.35784/bud-arch.2444>.
- [37] A. Owda, J. Balsa-Barreiro, D. Fritsch, Methodology for digital preservation of the cultural and patrimonial heritage: generation of a 3D model of the Church St. Peter and Paul (Calw, Germany) by using laser scanning and digital photogrammetry, Sens. Rev. 38 (3) (2018) 282–288, <https://doi.org/10.1108/SR-06-2017-0106>.
- [38] L. Guo, X. Deng, Y. Liu, H. He, H. Lin, G. Qiu, et al., Extraction of dense urban buildings from photogrammetric and LiDAR point clouds, IEEE Access 9 (2021) 111823–111832, <https://doi.org/10.1109/ACCESS.2021.3102632>.
- [39] X. Pu, S. Gan, X. Yuan, R. Li, Feature analysis of scanning point cloud of structure and research on hole repair technology considering space-ground multi-source 3D data acquisition, Sensors 22 (24) (2022), <https://doi.org/10.3390/s22249627>.
- [40] C. Sun, G. Che, X. Dong, R. Zou, L. Feng, X. Ding, Review on algorithm for fusion of oblique data and radar point cloud, in: Communications, Signal Processing, and Systems 2024, Springer Nature Singapore, Singapore, 2024, https://doi.org/10.1007/978-981-99-7502-0_58.
- [41] P. van Oosterom, S. van Oosterom, H. Liu, R. Thompson, M. Meijers, E. Verbree, Organizing and visualizing point clouds with continuous levels of detail, ISPRS J. Photogramm. Remote Sens. 194 (2022) 119–131, <https://doi.org/10.1016/j.isprsjprs.2022.10.004>.
- [42] D. Billi, V. Croce, M.G. Bevilacqua, G. Caroti, A. Pasqualetti, A. Piemonte, et al., Machine learning and deep learning for the built heritage analysis: laser scanning and UAV-based surveying applications on a complex spatial grid structure, Remote Sens 15 (8) (2023), <https://doi.org/10.3390/rs15081961>.
- [43] G.E. Gaong, A.N. Idris, C.L. Lau, A.A. Ab Rahman, W.M.S. Wan Mohamed Sabri, A. H. Abdul Jalil, Comparative evaluation of 3D building model using UAV photogrammetry and terrestrial laser scanner (TLS), Built Environ. J. 22 (1) (2025) 86–104, <https://doi.org/10.24191/bej.v22i1.1066>.
- [44] Y. Cui, Q. Li, B. Yang, W. Xiao, C. Chen, Z. Dong, Automatic 3-D reconstruction of indoor environment with Mobile laser scanning point clouds, IEEE J. Select. Top. Appl. Earth Observ. Remote Sens. 12 (8) (2019) 3117–3130, <https://doi.org/10.1109/JSTARS.2019.2918937>.
- [45] D. Moullou, R. Vital, S. Sylaiou, L. Ragia, Digital tools for data acquisition and heritage management in archaeology and their impact on archaeological practices, Heritage 7 (1) (2024) 107–121, <https://doi.org/10.3390/heritage7010005>.
- [46] V. Pouloupoulos, M. Wallace, Digital technologies and the role of data in cultural heritage: the past, the present, and the future, Big Data Cogn. Comp. 6 (3) (2022), <https://doi.org/10.3390/bdcc6030073>.
- [47] G. Lugo, R. Chauhan, I. Cheng, Exploring terrestrial point clouds with Google Street View for discovery and fine-grained catalog of urban objects, in: 2023 IEEE International Symposium on Multimedia (ISM), IEEE, 2023, <https://doi.org/10.1109/ISM58783.2023.00050>.
- [48] M. Berger, A. Tagliasacchi, L.M. Seversky, P. Alliez, G. Guennebaud, J.A. Levine, et al., A survey of surface reconstruction from point clouds, in: Computer Graphics Forum, Wiley Online Library, 2017, <https://doi.org/10.1111/cgf.12802>.
- [49] E. Alexiou, E. Upenik, T. Ebrahimi, Towards subjective quality assessment of point cloud imaging in augmented reality, in: 2017 IEEE 19th International Workshop on Multimedia Signal Processing (MMSP); 2017 16–18 Oct, 2017, <https://doi.org/10.1109/MMSP.2017.8122237>.
- [50] S. Lindholm, M. Falk, E. Sundén, A. Bock, A. Ynnerman, T. Ropinski, Hybrid data visualization based on depth complexity histogram analysis, Comp. Graph. Forum 34 (1) (2015) 74–85, <https://doi.org/10.1111/cgf.12460>.
- [51] M. Wu, T. Chen, K. Zhang, Z. Jing, Y. Han, M. Chen, et al., An efficient visualization method for polygonal data with dynamic simplification, ISPRS Int. J. Geo Inf. 7 (4) (2018) 138, <https://doi.org/10.3390/ijgi7040138>.
- [52] A. Tewari, J. Thies, B. Mildenhall, P. Srinivasan, E. Tretschk, W. Yifan, et al., Advances in neural rendering, in: Computer Graphics Forum, Wiley Online Library, 2022, <https://doi.org/10.1145/3450508.3464573>.
- [53] S.K. Baduge, S. Thilakarathna, J.S. Perera, M. Arashpour, P. Sharafi, B. Teodosio, et al., Artificial intelligence and smart vision for building and construction 4.0: machine and deep learning methods and applications, Autom. Constr. 141 (2022) 104440, <https://doi.org/10.1016/j.autcon.2022.104440>.
- [54] A.J. Paul, S. Ghose, K. Aggarwal, N. Nethaji, S. Pal, A.D. Purkayastha, Machine learning advances aiding recognition and classification of Indian monuments and landmarks, in: 2021 IEEE 8th Uttar Pradesh Section International Conference on Electrical 2021, Electronics and Computer Engineering (UPCON), Nov. 2021, pp. 11–13, <https://doi.org/10.1109/UPCON52273.2021.9667619>.
- [55] M. Andriasyan, J. Moyano, J.E. Nieto-Julián, D. Antón, From point cloud data to building information modelling: an automatic parametric workflow for heritage, Remote Sens. [Internet] 12 (7) (2020), <https://doi.org/10.3390/rs12071094>.
- [56] J. Moyano, I. Gil-Arízón, J.E. Nieto-Julián, D. Marín-García, Analysis and management of structural deformations through parametric models and HBIM workflow in architectural heritage, J. Build. Eng. 45 (2022) 103274, <https://doi.org/10.1016/j.job.2021.103274>.

- [57] J. Moyano, E. Carreño, J.E. Nieto-Julían, I. Gil-Arizón, S. Bruno, Systematic approach to generate historical building information modelling (HBIM) in architectural restoration project, *Autom. Constr.* 143 (2022) 104551, <https://doi.org/10.1016/j.autcon.2022.104551>.
- [58] T. Penjor, S. Banihashemi, A. Hajirasouli, H. Golzad, Heritage building information modeling (HBIM) for heritage conservation: framework of challenges, gaps, and existing limitations of HBIM, *Digit. Appl. Archaeol. Cultural Heritage* 35 (2024) e00366, <https://doi.org/10.1016/j.daach.2024.e00366>.
- [59] A. Crisan, M. Pepe, D. Costantino, S. Herban, From 3D point cloud to an intelligent model set for cultural heritage conservation, *Heritage* 7 (3) (2024) 1419–1437, <https://doi.org/10.3390/heritage7030068>.
- [60] X. Zhao, A Virtual Reality Application: Creating an Alternative Immersive Experience for Dunhuang Mogao, Duke University, Cave visitors, 2023.
- [61] N.K. Surendran, X.W. Xu, O. Stead, H. Silyn-Roberts, Contemporary technologies for 3D digitization of Maori and Pacific Island artifacts, *Int. J. Imaging Syst. Technol.* 19 (3) (2009) 244–259, <https://doi.org/10.1002/ima.20202>.
- [62] A. Dalal, D. Hagen, K.G. Robbersmyr, K.M. Knausgård, Gaussian splatting: 3D reconstruction and novel view synthesis: a review, *IEEE Access* 12 (2024) 96797–96820, <https://doi.org/10.1109/ACCESS.2024.3408318>.
- [63] P. Clini, R. Nespeca, R. Angeloni, L. Coppetta, 3D representation of architectural heritage: A comparative analysis of NeRF, Gaussian splatting, and SfM-MVS reconstructions using low-cost sensors, in: *Int Arch Photogramm Remote Sens Spatial Inf Sci*, Copernicus Publications, 2024, pp. 93–99, <https://doi.org/10.5194/isprs-archives-XLVIII-2-W8-2024-93-2024>.
- [64] A. Basso, F. Condorelli, A. Giordano, S. Morena, M. Perticarini, Evolution of rendering based on radiance fields: the Palermo case study for a comparison between NeRF and Gaussian splatting, *Int. Arch. Photogramm. Remote. Sens. Spat. Inf. Sci.* (2024) 57–64, <https://doi.org/10.5194/isprs-archives-XLVIII-2-W4-2024-57-2024>.
- [65] V. Croce, G. Caroti, L. De Luca, A. Piemonte, P. Véron, Neural radiance fields (NeRF): review and potential applications to digital cultural heritage, *Int. Arch. Photogramm. Remote. Sens. Spat. Inf. Sci.* (2023) 453–460, <https://doi.org/10.5194/isprs-archives-XLVIII-M-2-2023-453-2023>.
- [66] O. Jamil, A. Brennan, Immersive heritage through Gaussian splatting: a new visual aesthetic for reality capture, *Front. Comp. Sci.* 7 (2025) 2025, <https://doi.org/10.3389/fcomp.2025.1515609>.
- [67] J. Luo, T. Huang, W. Wang, W. Feng, A review of recent advances in 3D Gaussian splatting for optimization and reconstruction, *Image Vis. Comput.* 151 (2024) 105304, <https://doi.org/10.1016/j.imavis.2024.105304>.
- [68] H. Van Dijk, *Twentieth-Century Architecture in the*, 010 Publishers, Netherlands, 1999. Available from: <https://www.worldcat.org/title/42046340>.
- [69] A. Kirillov, E. Mintun, N. Ravi, H. Mao, C. Rolland, L. Gustafson, editors., et al., Segment anything, in: *Proceedings of the IEEE/CVF International Conference on Computer Vision*, 2023, <https://doi.org/10.48550/arXiv.2304.02643>.
- [70] M.W. Ahmed, A. Jalal, Robust object recognition with genetic algorithm and composite saliency map, in: *2024 5th International Conference on Advancements in Computational Sciences (ICACS)*, IEEE, 2024, <https://doi.org/10.1109/ICACS60934.2024.10473285>.
- [71] M. Schwab, A. Mayr, M. Haltmeier, Deep Gaussian mixture model for unsupervised image segmentation, *arXiv* (2025), <https://doi.org/10.48550/arXiv.2404.12252> preprint arXiv:2404.122522024.
- [72] H. Kim, I.-K. Lee, Is 3DGS useful? Comparing the effectiveness of recent reconstruction methods in VR, in: *2024 IEEE International Symposium on Mixed and Augmented Reality (ISMAR)*, IEEE, 2024, <https://doi.org/10.1109/ISMAR62088.2024.00021>.
- [73] J. Kang, N. Chen, M. Li, S. Mao, H. Zhang, Y. Fan, et al., A point cloud segmentation method for dim and cluttered underground tunnel scenes based on the segment anything model, *Remote Sens* 16 (1) (2024), <https://doi.org/10.3390/rs16010097>.
- [74] K. Yu, L. Ji, X. Zhang, Kernel nearest-neighbor algorithm, *Neural. Process. Lett.* 15 (2002) 147–156, <https://doi.org/10.1023/A:1015244902967%E3%80%82>.
- [75] J. Cui, J. Cao, F. Zhao, Z. He, Y. Chen, Y. Zhong, et al., LetsGo: large-scale garage modeling and rendering via LiDAR-assisted Gaussian primitives, *ACM Trans. Graph.* 43 (6) (2024), <https://doi.org/10.1145/3687762>. Article 172.
- [76] C. Peng, Y. Tang, Y. Zhou, N. Wang, X. Liu, D. Li, et al., BAGS: blur agnostic Gaussian splatting through multi-scale kernel modeling, in: *Computer Vision – ECCV 2024 2025*, Springer Nature Switzerland, Cham, 2025, https://doi.org/10.1007/978-3-031-72989-8_17.
- [77] H. Wang, M. Li, A new era of indoor scene reconstruction: a survey, *IEEE Access* 12 (2024) 110160–110192, <https://doi.org/10.1109/ACCESS.2024.3440260>.
- [78] M.S. Ali, C. Zhang, M. Cagnazzo, G. Valenzise, E. Tartaglione, S.-H. Bae, Compression in 3D Gaussian splatting: a survey of methods, trends, and future directions, *arXiv* (2025), <https://doi.org/10.48550/arXiv.2502.19457> preprint arXiv:2502.19457.